International Journal of Sciences: Basic and Applied Research (IJSBAR)

ISSN 2307-4531
(Print & Online)

http://gssrr.org/index.php?journal=JournalOfBasicAndApplied

Numerical Assessment of the Thermomechanical Properties of the N_iT_i Shape Memory Alloy

Belkacem Kada*

Department of Aeronautical Engineering, King Abdulaziz University, P O Box 80204, Jeddah, 21589 KSA

Email: bkada@ kau.edu.sa; Belkacemkad@hotmail.com

Abstract

The paper presents a numerical assessment and characterization of Shape Memory Alloys (SMAs) thermomechanical behavior using an internal variable approach-based constitutive law. A simulation study is conducted to reveal the influence of the key intrinsic properties such as shape memory effect, pseudoelastic effect, hysteresis loop, and non-constant material functions on the loading capacity and thermal actuation of SMAs. The effects of initial conditions, residual strains, and high temperatures on the behavior of SMAs are studied through several thermomechanical loading-unloading scenarios. The results give useful indications on the capability of SMA materials to fully recover large strains under thermal activation, to change their properties reversibly through phase transformation, and to serve as actuator systems for engineering control applications.

Keywords: Hysteresis models; pseudoelastic effect; constitutive modelling; metastable phase; shape memory alloys; two-way shape memory effect.

1. Introduction

Since discovered in 1938 [1], the Shape Memory Alloy (SMA) materials have been receiving increasingly attention and studies with growing effort from scientific community and engineers.

---

* Corresponding author.

The particular properties of SMA materials such as Shape Memory Effect (SME), Superelasticity (SE), self-accommodating martensite transformation, and thermal actuation, make these materials more attractive for the design of smart structures, innovative devices, and new intelligent materials. Nowadays, SMA materials are being used in cutting-edge technologies such as airplanes and rockets, automatic flow control, wireless communications, and biomedical applications [2-5]. From thermomechanical point of view, SMAs have outstanding characteristics such as large load capacity, extremely large recovery strains, enhanced fatigue performance, force bearing, and phase transformation-dependent elastic and thermal properties. These characteristics allow the integration at high degree of SMA materials into the actuation of intelligent systems [5-10]. Over the last few decades, many phenomenological constitutive models have been developed and experimental characterizations have been conducted to address the behaviors observed in SMA materials [11-17]. Among these investigations, the internal variable-based model given in [14] is the most popular and widely used on engineering due to the following advantages

- Separation of martensite fraction into stress-induced and temperature-induced fractions.
- Extensibility to materials for which the properties are functions of the state variables.
- Use of common engineering variables and measurable properties.
- Adaptability to any new experimental evidences.
- Well suitable for engineering design and practical applications.

It is worth noting that the model presented in [14] has been the subject of many interesting recent investigations [18-21]

To clearly understand and more effectively simulate the characteristics of SMA materials, this paper presents a detailed analysis of SMA transformations using Brinson's phenomenological model [14] with consideration of more critical analysis cases. The emphasis in this study is on the inherent characteristics of SMAs such as SME, SE, hysteresis loop, and non-constant material functions. To perform numerical simulations, the Nitinol alloy ($Ni_{55}Ti$) SMA is used. Since discovered in 1963 [22], the Nitinol-Ti SMA has been largely used in many exciting and innovative engineering applications and a large number of theoretical and experimental studies have been conducted to characterize and reveal the key characteristics of this metastable phase material [22-26]. These investigations show that NiTi SMA exhibits exceptional characteristics that can be used for development of novel actuator systems.

2. SMA Constitutive Behavior and Rheological Laws

2.1. Background

By virtue of their various characteristics, SMA materials can recover large residual permanent strains (up to 10%) in a thermomechanical loading/unloading path as shown in Figure 1.

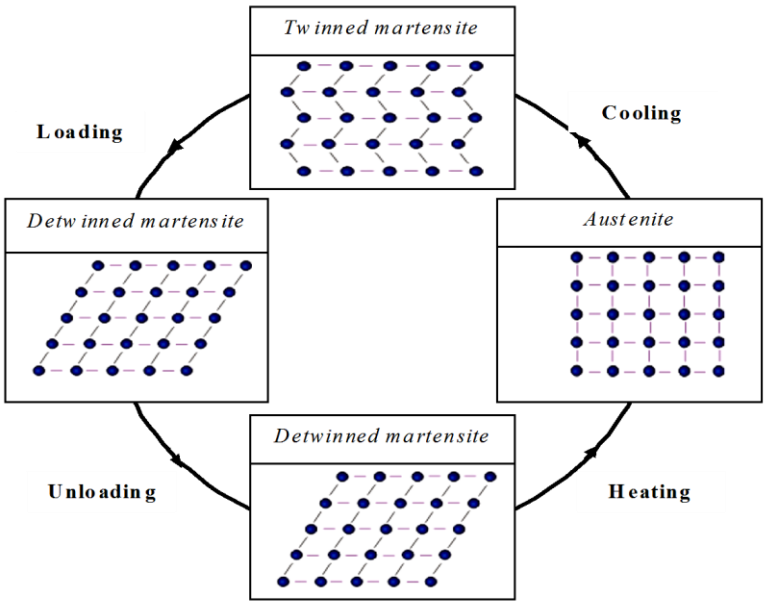

Figure 1: Schematic of phase transformation of SMA

Two main temperature-dependent stable phase transformations characterize the behavior of SMA: low temperature phase "martensite" and high temperature phase "austenite". These phase transformations are driven by four stress-dependent temperatures: martensite start M_s, martensite finish M_f, austenite start A_s and austenite finish A_f. Depending on the value of the applied heating temperature with respect to the material transformation temperatures, the behavior of SMA can be completely understood using the temperature T, the stress σ, and the strain ε, as material state variables. This behavior is graphically illustrated in Figure 2. For more details about phase transformation, reorientation process, strain mechanisms, and microstructural evolutions of SMA, the reader is referred to [14,27-31].

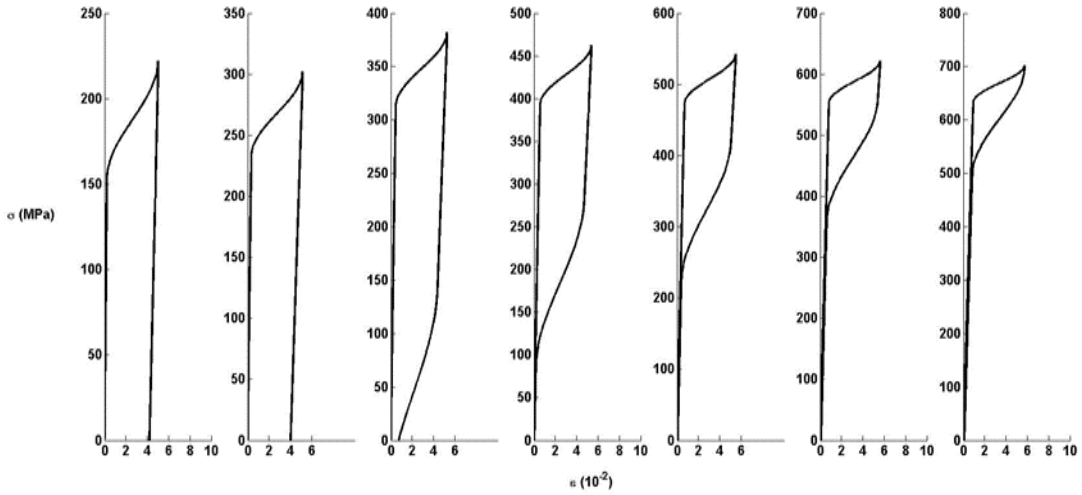

Figure 2: Stress-strain curves of $Ni_{55}Ti$ SMA during conversion at different isothermal temperatures

2.2. Thermomechanical Behavior of Shape Memory Alloy Materials

According to Tanaka's argument, the thermomechanical behavior of SMAs can be efficiently described using three material state variables, i.e. mechanical strain, thermal temperature, and stage transformation. Assuming that the thermomechanical elastic properties and phase transformation functions are constant, Tanaka's constitutive model for SMA materials is written in the rate form [32]

$$d\sigma = E(\varepsilon,\xi,T)d\varepsilon + \Omega(\varepsilon,\xi,T)d\xi + \Theta(\varepsilon,\xi,T)dT \quad (1)$$

where the state variables σ, ε, ξ, and T are the stress, strain, martensite volume fraction, and temperature of the material, respectively. The material coefficients E, Ω, and Θ denote the elastic modulus, phase transformation, and thermoelastic property (thermal expansion), respectively. In the original form of the model (1), all the material coefficients are supposed to be constant yielding to a linear SMA constitutive model. Assuming that the SMA has a maximum recoverable residual strain ε_L and using the model (1) to transform an austenite phase $(\sigma_0 = \varepsilon_0 = \xi_0 = 0)$ to a complete martensite phase $(\sigma = 0, \varepsilon = \varepsilon_L, \xi = 1)$ under the isothermal loading $(T = T_0,\ M_s < T < A_s)$, the phase transformation tensor Ω is proportional to E

$$\Omega = -\varepsilon_L E \quad (2)$$

In the general expression of the model (1), the material coefficients are defined as the second-derivative functions of the Helmholtz free energy [14],

$$\begin{cases} E(\varepsilon,\xi,T) = \rho_0 \frac{\partial^2 \Phi}{\partial \varepsilon^2} \\ \Omega(\varepsilon,\xi,T) = \rho_0 \frac{\partial^2 \Phi}{\partial \varepsilon\, \partial \xi} \\ \Theta(\varepsilon,\xi,T) = \rho_0 \frac{\partial^2 \Phi}{\partial \varepsilon\, \partial T} \end{cases} \quad (3)$$

Based upon experimental studies presented in [33], it was found that the material coefficients of a SMA are dependent on the state ξ. From experimental evidences, it was fund that for one-dimensional SMA Young's modulus has a strong dependence on ξ [13,33,34]. Based upon the separation principle, a linear form is proposed [13,34]

$$E(\varepsilon,\xi,T) \equiv E(\xi) = E_a + \xi(E_m - E_a) \quad (4)$$

where E_a and E_m are the Young's moduli for 100% austenite and 100% martensite, respectively. With lack of firm experimental evidences about the variation of the material functions Ω and Θ with respect to the state variables, the following relationships for the variation of Ω and Θ with respect to ξ were proposed

$$\begin{cases} \Omega(\varepsilon,\xi,T) \equiv \Omega(\xi) = -\varepsilon_L E_a - \varepsilon_L \xi (E_m - E_a) \\ \Theta(\varepsilon,\xi,T) \equiv \Theta(\xi) = \Theta_a + \xi(\Theta_m - \Theta_a) \end{cases} \quad (5)$$

or equivalently

$$\begin{cases} \Omega(\xi) = -\varepsilon_L \mathrm{E}(\xi) \\ \Theta(\xi) = \alpha(\xi)\mathrm{E}(\xi) \end{cases} \quad (6)$$

In order to extend the constitutive law (1) to simultaneously represent the shape memory and the pseudoelasticity effects, the state ξ is subdivided into multi-variant temperature-induce ξ_T and single-variant stress-induced ξ_s martensite volume fractions [14]

$$\xi = \xi_s - \xi_T \quad (7)$$

The integration of the model (1)-(5) with $(\sigma_0, \varepsilon_0, \xi_0, T_0)$ as initial state yields the following final constitutive equation for SMA behavior

$$\sigma = \sigma_0 + E(\xi)\varepsilon - E(\xi_0)\varepsilon_0 + \Omega(\xi)\xi_s - \Omega(\xi_0)\xi_{s0} + \Theta(T - T_0) \quad (8)$$

The different fractions in (7) are supposed to be functions of stress and temperature and can be determined for both martensite and austenite phases. Using the empirically based cosine model formulated from phase equilibrium and transformation kinetics [13], the evolutions of the fractions $\xi_s$and ξ_a with respect to temperature and stress are given by the following transformation equations [14]

Conversion to detwinned martensite

For $T > M_s$ and $\sigma_s^{cr} + C_M(T - M_s) < \sigma < \sigma_f^{cr} + C_M(T - M_s)$

$$\begin{aligned} \xi_s &= \left(\frac{1-\xi_{s0}}{2}\right) cos\left\{\frac{\pi}{\sigma_s^{cr} - \sigma_f^{cr}}\left[\sigma - \sigma_f^{cr} - C_M(T - M_s)\right]\right\} + \frac{1+\xi_{s0}}{2} \\ \xi_T &= \xi_{T0} - \frac{\xi_{T0}}{1-\xi_{T0}}(\xi_s - \xi_{s0}) \end{aligned} \quad (9)$$

For $T < M_s$ = and $\sigma_s^{cr} < \sigma < \sigma_f^{cr}$

$$\begin{aligned} \xi_s &= \left(\frac{1-\xi_{s0}}{2}\right) cos\left[\frac{\pi}{\sigma_s^{cr} - \sigma_f^{cr}}\left(\sigma - \sigma_f^{cr}\right)\right] + \frac{1+\xi_{s0}}{2} \\ \xi_T &= \xi_{T0} - \frac{\xi_{T0}}{1-\xi_{T0}}(\xi_s - \xi_{s0}) + \Delta_{T\xi} \end{aligned} \quad (10)$$

where

$$\Delta_{T\xi} = \begin{cases} \left(\frac{1-\xi_{T0}}{2}\right)\left\{cos\left[a_M\left(T - M_f\right)\right] + 1\right\}, & for\ M_f < T < M_s\ and\ T < T_0 \\ 0, & else \end{cases} \quad (11)$$

Conversion to austenite

For $T > A_s$ and $C_A\left(T - A_f\right) < \sigma < C_A(T - A_s)$

$$\begin{cases} \xi = \frac{\xi_{s0}}{2}\left\{cos\left[a_A\left(T - A_s - \frac{\sigma}{C_A}\right)\right] + 1\right\} \\ \xi_s = \xi_{s0} - \frac{\xi_{s0}}{\xi_0}(\xi_0 - \xi) \\ \xi_T = \xi_{T0} - \frac{\xi_{T0}}{\xi_0}(\xi_0 - \xi) \end{cases} \quad (12)$$

In this formulation C_M and C_A are material properties which describe the relationship of temperature and critical stress to induce transformation, and the parameters a_M and a_T are defined by

$$a_M = \frac{\pi}{M_s - M_f}, \quad a_A = \frac{\pi}{A_f - A_s} \quad (13)$$

3. SMA Constitutive Behavior and Rheological Laws

In order to understand the outstanding properties of SMA materials, a series of numerical simulations were performed using different thermomechanical loading scenarios. The SMA material used for simulation is $Ni_{55}Ti$ where the material properties are listed in Table 1 [14].

Table 1: Material properties of the $Ni_{55}Ti$ SMA

Transformation Temperatures	Transformation Stresses/Constants	Moduli/ Constants
$M_s = 18.4°C$	$\sigma_s^{cr} = 100\ MPa$	$E_a = 67x10^3\ GPa$
$M_f = 9\,°C$	$\sigma_f^{cr} = 170\ MPa$	$E_m = 26.3x10^3\ GPa$
$A_s = 34.5\,°C$	$C_M = 8M\ Pa/°C$	$\Theta_0 = 0.55\ MPa/°C$
$A_f = 49\,°C$	$C_A = 13.8\,MPa/°C$	$\varepsilon_L = 0.067$

3.1. Conversion to austenite

Simulation 1: In this simulation, the temperature of a SMA material was increased from T_0=20°C to T=80°C above A_f to recover from a residual stress of ε_0=2% considering two different loading cases: σ=0MPa and σ=150MPa . The simulation was performed using the conditions given in Table 2.

Figures 3a and Figure 3b demonstrate the inverse transformation to austenite and the free strain recovery of the material, respectively. The evolutions of thermomechanical characteristics of the SMA material during the transformation are shown in Figure 4.

Table 2: Initial conditions for the conversion to austenite simulation

Parameter	Value
T_0	$20°C$
T	$80°C$
σ_0	[0, 150] MPa
ε_0	0.02
ξ_{T0}	0.5
ξ_{S0}	0.02/0.067=0.2985

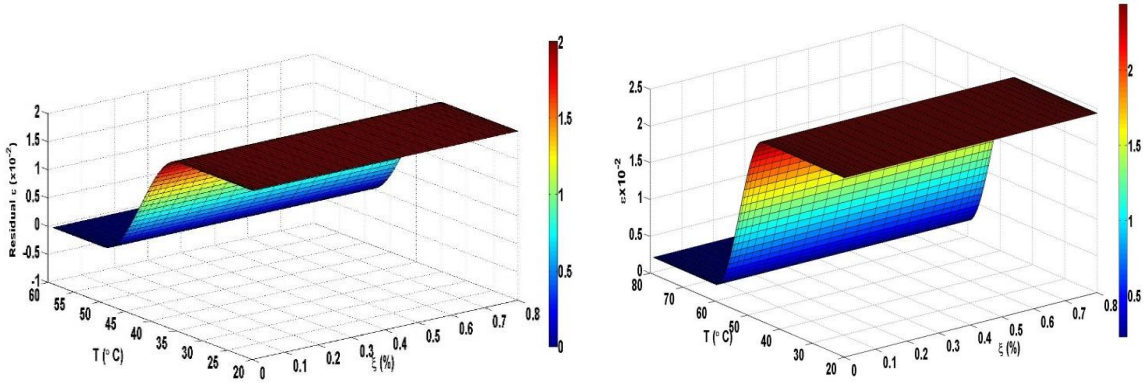

$\sigma = 0MPa$ $\sigma = 150MPa$

(a) (b)

Figure 3: Free strain recovery of SMA material in inverse transformation to austenite with two different loading conditions: (a) and (b) free strain recovery

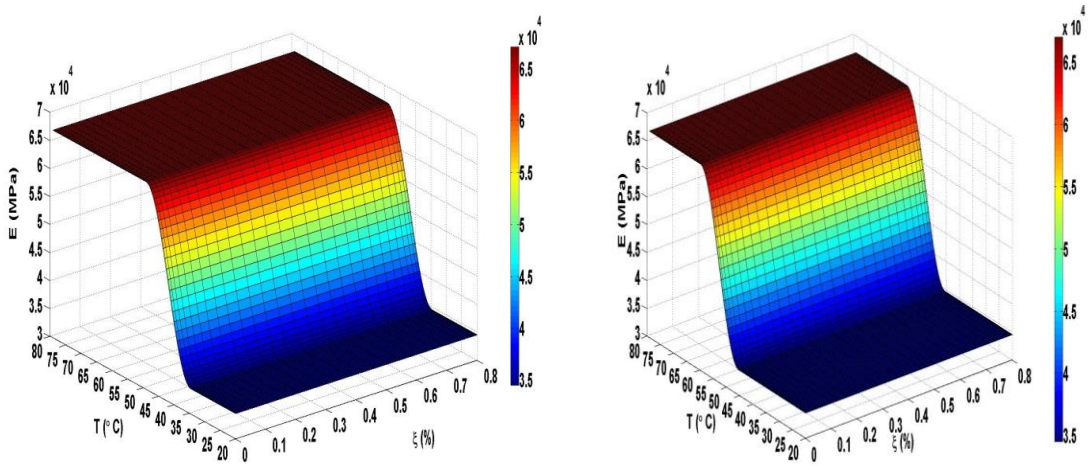

$\sigma = 0MPa$ $\sigma = 150MPa$

(a) (b)

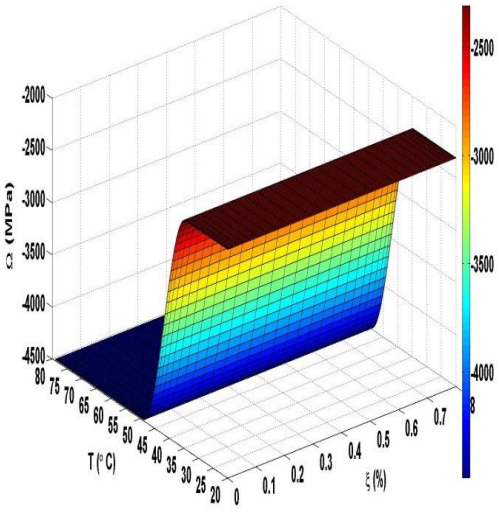

$\sigma = 0MPa$

(c)

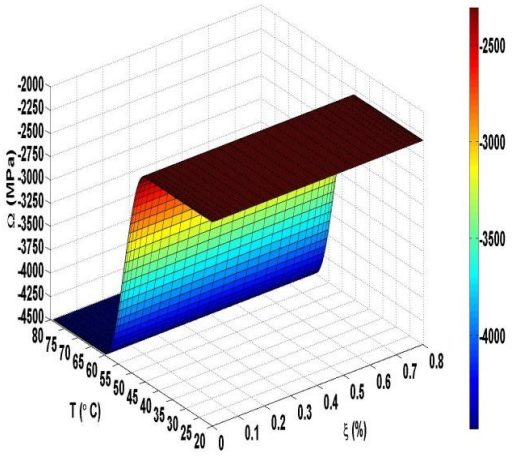

$\sigma = 150MPa$

(d)

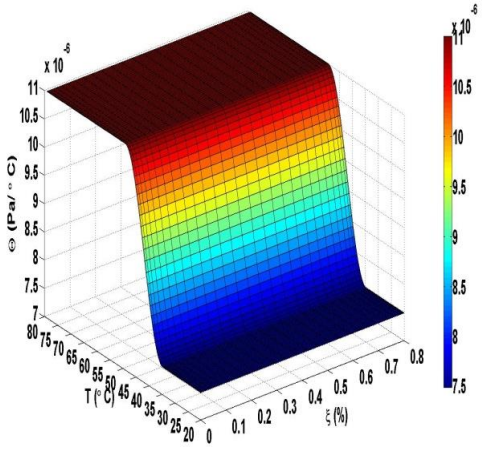

$\sigma = 0MPa$

(e)

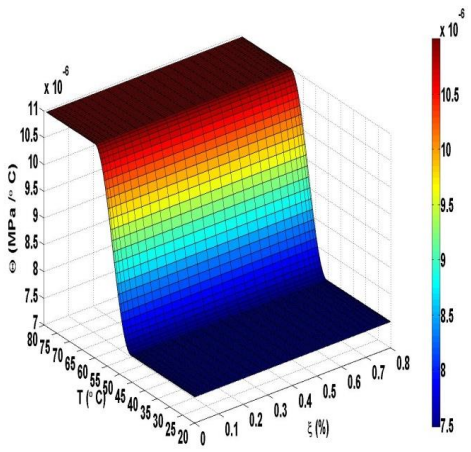

$\sigma = 150MPa$

(f)

Figure 4: SMA properties free strain recovery in inverse transformation to austenite with two different loading conditions: (a) and (b) elastic modulus; (c) and ((d) phase transformation; (e) and (f) thermal expansion

Increasing the temperature T above the austenite-finish temperature A_f the SMA completely recovers initial residual stresses $\varepsilon_0 < \varepsilon_L$ at $\sigma = 0$ as shown in Figure 4. If the material is loaded with $\sigma > 0$, the final residual strain ε_f is very low than the initial strain $\varepsilon_i = \varepsilon_0 + \varepsilon_l$ where ε_l is the strain induced by σ. In case of $\sigma_s^{cr} = 100\ MPa < \sigma = 150\ MPa < \sigma_f^{cr} = 170\ MPa$, the total initial residual strain is $\varepsilon_i = 0.02435\ > \varepsilon_0$, and the

final recovery strain is $\varepsilon_f = 0.00227$.

3.2. Conversion to detwinned martensite: pseudoelastic and shape memory effects

A. Partial pseudoelastic recovery and complete hysteresis loop

Simulation 2: In this simulation, the thermomechanical response of the SMA material was computed for a complete loading/unloading path. The isothermal thermomechanical uniaxial loadings were performed at different temperatures from $T > M_s$ to $T > A_f$. The simulation 2 was run using an initial residual strain of $\varepsilon_0 = 2\%$ (non-zero stress-induced martensite variable) and $T_0 = 0°C$. A complete hysteretic loop of SMA is illustrated in Figure 5 and the calculated stress-stain curves are shown in Figure 6.

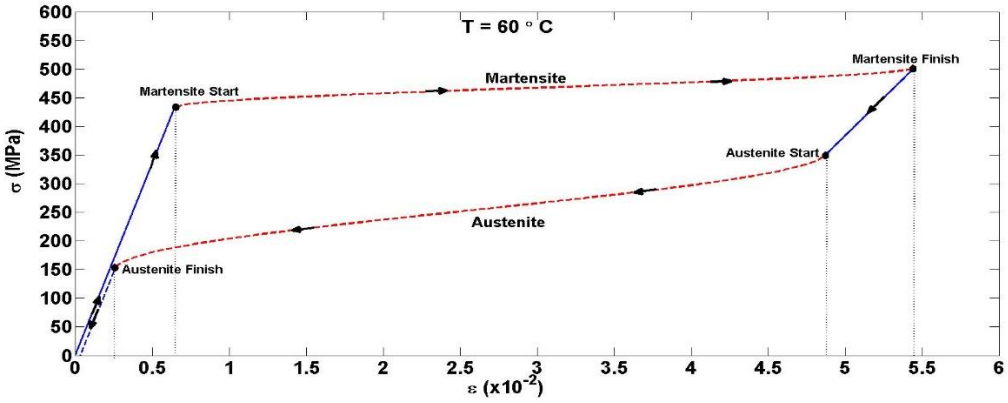

Figure 5: A complete SMA hysteresis loop

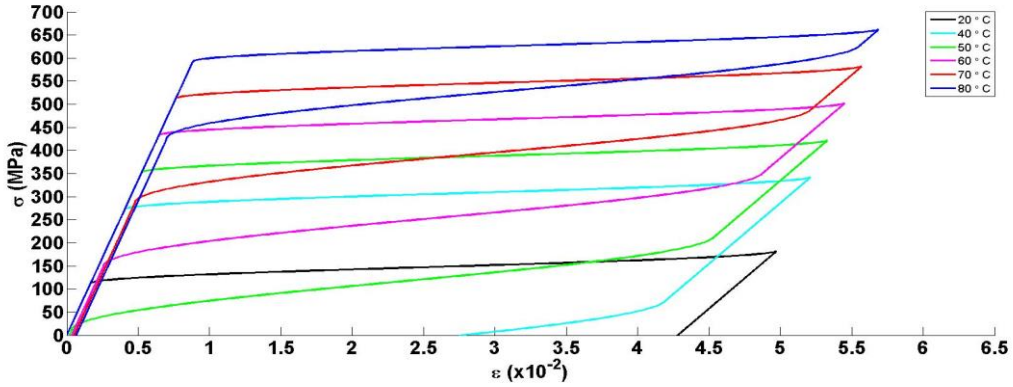

Figure 6: SMA pseudoelastic recovery and shape memory effect under isothermal uniaxial loading

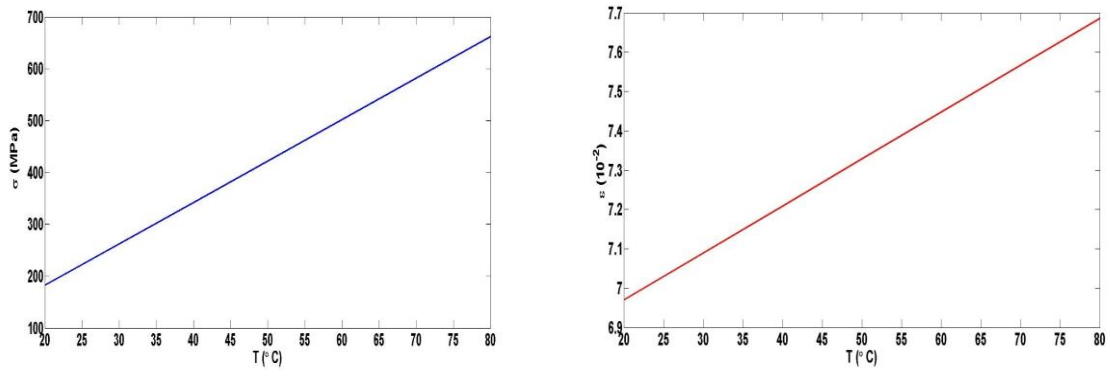

(a) (b)

Figure 7: Loading capacity of SMA material versus isothermal temperature (a) stress loading, and (b) strain growth

In Figure 5, a complete hysteresis response was obtained for a temperature $T = 60°C > A_f$. Gradually increasing the load from zero, the austenite SMA transforms to a detwinned martensite until saturation, and then it recovers, during unloading, from residual strains through inverse transformation to austenite. From Figure 6, it can be seen clearly that:

- Above the austenite-finish temperature, the effect of the shape memory is complete and the SMA exhibits a complete hysteresis loop.
- Below the austenite-finish temperature, the effect of the shape memory is partial (partial residual strain recovery).
- Above the austenite-finish temperature, the SMA recovers all residual strains.
- Above the austenite-start temperature, the pseudoelastic recovery effect starts.
- The stress martensite-start magnitude rises with the transformation temperature.
- The capacity loading during hysteresis loop deceases as temperature increases above A_s.
- At high temperature above A_f, SMA recovers large strains and maintains linear properties.

Figure 7 shows that the loading capacity and recovered strain of SMAs are monotonically increasing functions versus isothermal temperature.

B. Conversion to complete detwinned martensite

Simulation 3: a third simulation was performed to show the capability of the SMA to transform to a complete detwinned martensite at a temperature $T < M_s$. The third simulation was run using the initial conditions shown in Table 3 for different temperatures $T \in 0,18]°C$.

Table 3: Initial conditions for the conversion to martensite simulation with $T < M_s$

Parameter	Value
T_0	$0°C$
ε_0	0
σ_0	0 MPa
ξ_{T0}	1
ξ_{S0}	0

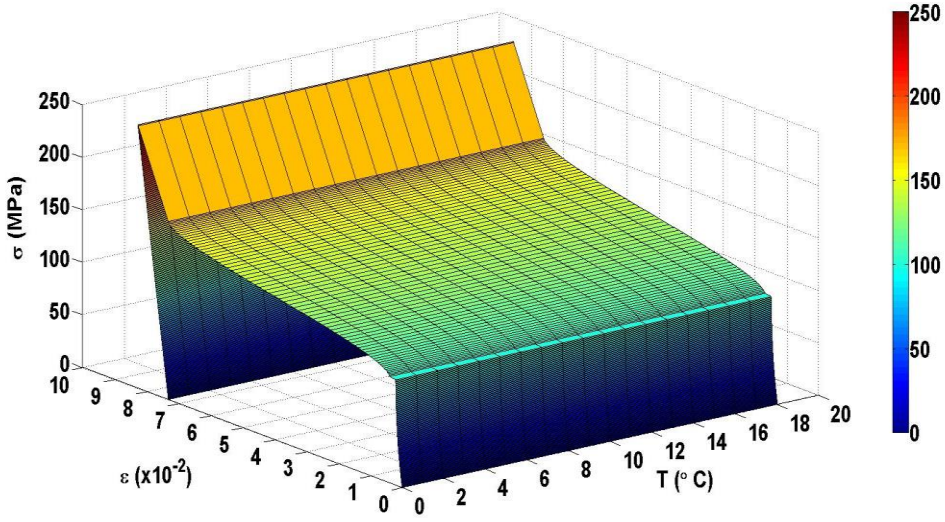

Figure 8: Shape memory effect during a complete martensite transformation

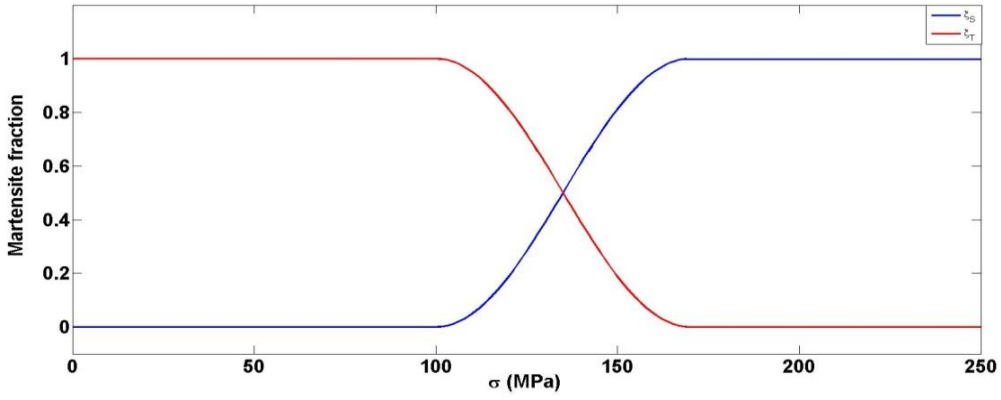

Figure 9: Martensite fractions vs. stress for loading-unloading path

4. Conclusion

A numerical study was presented to understand the complex and interesting thermomechanical behavior of SMAs and to assess the useful properties of these materials on designing smart structures and devices such as

sensors, actuators, etc. The results of the present study show that SMAs can fully recover free large residual strains as well as considerably reduce permanent strains under mechanical loading. The maximum loading temperature and stress were found to be $80°C$ and $650\ MPa$, respectively. In addition, it was shown that SME and thermal activation are useful properties for application of SMAs as actuators in the field of engineering practice. Ongoing investigations will extend the analysis to SMA-based actuation systems and time-response of the hysteresis loop.

Acknowledgments

This Project was funded by the Deanship of Scientific Research (DSR), King Abdulaziz University, Jeddah. The authors, therefore, acknowledge with thanks DSR technical and financial support.

References

[1] Greninger B., and Mooradian V.G., Strain transformation in metastable beta copper-zinc and beta copper-tin alloys, Transactions of the Metallurgical Society of AIME, vol. **128,** (1939), 337–368.

[2] Duerig T.W., Melton K.N., Stoeckel D., and Wayman C.M., Engineering aspects of shape memory alloys, Butterworth- Heinemann, London, (1990).

[3] Lagoudas D., Shape memory alloys: modeling and engineering applications, 1st edition. Springer, New York, (2008).

[4] Yoneyama T. , and Miyazaki S., Shape memory alloys for biomedical applications, Woodhead Publishing, England, (2009).

[5] Yamauchi K., Ohkata I., Tsuchiya K., and Miyazaki S., Shape Memory and Superelastic Alloys: Technologies and Applications, Woodhead Publications, Cambridge, (2011).

[6] Chen S., Craft W.J., Song D.Y., Nonlinear adaptive control of dynamic systems driven by shape memory alloy (SMA) actuators, In: IMECE Mechanical Systems and Control, vol. **11,** (2009) ,767–774.

[7] Benafan O., Brown J., Calkins F.T., Kumar P., Stebner A.P., Turner T. L. , Vaidyanathan R., Webster J., and Young M.L., Shape memory alloy actuator design: CASMART collaborative best practices and case studies, International Journal of Mechanics and Materials Design, vol. **10,** (2014), 1–42.

[8] Nath, T., Raut, G., Kumar, A., Khatri, R. and Palani, I.A., Investigation on Laser assisted actuation of shape memory alloy based micro-valve, International Conference on Robotics, Automation, Control and Embedded Systems (RACE), Chennai, (2015), 1-6.

[9] Swapnil, S.S, Ariful I., Shape Memory Materials - Concepts, Recent Trends and Future Directions, 7th International Conference on Informatics, Electronics & Vision (ICIEV), July**,** (2018),.

[10] Prabu, S.S.M, Mithun R, Muralidharan, M., Tameshwer, N., Brolin, A., Akash, A., and Palani, A.I., Thermo-mechanical behavior of shape memory alloy spring actuated using novel scanning technique powered by ytterbium doped continuous fiber laser, Smart Materials and Structures, vol. **28**(4) 2019,

[11] Falk F., Ginzburg-Landau theory of static domain walls is Shape Memory Alloys, Zeitschrift für Physik B Condensed Matter, vol. **51,** (1983), 177-185.

[12] Brinson L.C., One-dimensional constitutive behavior of shape memory alloys: thermomechanical derivation with nonconstant material functions and redefined martensite internal variable, Journal of Intelligent Materials and Structures, vol. **4,** (1993), 229–242.

[13] Tanaka K., Nishimura F., Hayashi T., Tobushi H., and Lexcellent C., Phenomenological analysis on subloops and cyclic behavior in shape memory alloys under mechanical and/or thermal loads, Mechanics of Materials. vol. **19,** (1995), 281-292.

[14] Boyd J.G., and Lagoudas D.C., A thermodynamic constitutive model for the shape memory alloy materials. Part I. The monolithic shape memory alloy, International Journal of Plasticity. vol. **12,** (1996), 805-842.

[15] Sahli M.L., and Necib B., Characterisation and modelling of behaviour of a shape memory alloys, International Journal of Advanced Manufacturing Technology, vol. **70,** (2014), 1847-1857.

[16] Bryła, J., and Martowicz, A., Experimental and numerical assessment of the characteristics describing superelasticity in shape memory alloys – influence of boundary conditions, ITM Web of Conferences, vol. **15**(06007), (2017), 1-8.

[17] Huang, B., Hongwang, Lv., and Song, Y., Numerical Simulation and Experimental Study of a Simplified Force-Displacement Relationship in Superelastic SMA Helical Springs, Sensors (Basel). , **19**(50), 2019, 2-21.

[18] Brocca M., Brinson L.C., and Bazant Z., Three-dimensional constitutive model for shape memory alloys based on microplane model, Journal of Mechanics and Physics of Solids, vol. **50**(5)**,** (2002), 1051–1077.

[19] Arghavani J., Auricchio F., Naghdabadi R., Reali A., and Sohrabpour S., A 3-D phenomenological constitutive model for shape memory alloys under multiaxial loadings, International Journal of Plasticity, vol. **26**(7), (2010), 976–991.

[20] Auricchio F., Bonetti E., Scalet G., and Ubertini F., Theoretical and numerical modeling of shape memory alloys accounting for multiple phase transformations and martensite Reorientation, International Journal of Plasticity, vol. **59,** (2014), 30–54

[21] Sahli M.L., and Necib B., Characterisation and modelling of behaviour of a shape memory alloys, International Journal of Advanced Manufacturing Technology, vol. **70,** (2014),1847–1857.

[22] Buehler W.J., Gilfrich J.V., and Wiley R.C., Effect of low temperature phase changes on the mechanical properties of alloys near composition TiNi, Journal of Applied Physics, vol. **34**(5), (1963), 1475–1477.

[23] Zurbitu J., Santamarta R., Picornell C., Gan W.M., Brokmeier H.G., and Aurrekoetxea J, Impact fatigue behavior of superelastic NiTi shape memory alloy wires, Material Science and Engineering A, vol. **528**(2), (2010), 764–769.

[24] Antico F.C., Zavattieri P.D., Hector Jr L.G, Mance A., Rodgers W.R., and Okonski D.A., Adhesion of nickel-titanium shape memory alloy wires to thermoplastic materials: theory and experiments, Smart Material Structures, vol. **21**, (2012), 3035022.

[25] Zhang Y., Jiang S., Hu L. , and Liang Y., Deformation mechanism of NiTi shape memory alloy subjected to severe plastic deformation at low temperature, Material Science and Engineering A, vol. **559,** (2013), 607–614.

[26] Guida, M., Sellitto, A., Marulo, F., and Riccio, A., Analysis of the Impact Dynamics of Shape Memory Alloy Hybrid Composites for Advanced Applications, Materials, vol. **12(**153), 2019, 2-14.

[27] Tanaka K., Kobayashi S., and Sato Y., Thermomechanics of transformation pseudoelasticity and shape memory effect in alloys, International Journal of Plasticity, vol. **2,** (1986), 59-72.

[28] Birman V., Review of mechanics of shape memory alloy structures, Applied Mechanics Reviews, vol. **50-11,** (1997), 629-645.

[29] Lagoudas D.C., Entchev P.B., Popov P., Patoor E., Brinson L.C., and Gao X., Shape memory alloys,c. Part II: Modeling of polycrystals, Mechanics of Materials, vol. **38,** (2006), 430-462.

[30] Lagoudas D.C, Shape memory alloys: modeling and engineering applications, Springer: New York. (2008).

[31] Stebner A.P., Vogel S.C., Noebe R.D., Sisneros T.A., Clausen B., Brown D.W., Garg A., and Brinson L.C., Micromechanical quantification of elastic, twinning, and slip strain partitioning exhibited by polycrystalline, monoclinic nickel–titanium during large uniaxial deformations measured via in-situ neutron diffraction, Journal of the Mechanics and Physics of Solids, vol. **61,** (2013), 2302–2330.

[32] Tanaka K. and Nagaki S., A thermomechanical description of materials with internal variables in the process of phase transitions, Ingenieur-Archiv, vol. **51**(5), (1982), 287–299.

[33] Duerig T., and Melton K., Wide Hysteresis NiTiNb Alloys. The Martensitic Transformation in Science and Technology, DGM Informationsgesellschaft-Verlag, Oberursel, (1989).

[34] Tanaka K., and Iwasaki R., A phenomenological theory of transformation superplasticity, Engineering Fracture Mechanics, vol. **21**(4), (1985), 709–720.

[35] Sato Y., and Tanaka K., Estimation of Energy dissipation in Alloys due to Stress-induced martensite transformation, Res. Mechanica, vol. **23,** (1989), 381-393.